Journal of
Nanoscience and Nanotechnology
Vol. 11, 3141–3150, 2011

Mechanisms of Viscosity Increase for Nanocolloidal Dispersions

Tao Wang[1], Xinwei Wang[2,*], Zhongyang Luo[1,*], Mingjiang Ni[1], and Kefa Cen[1]

[1] State Key Laboratory of Clean Energy Utilization, Zhejiang University, Hangzhou, 310027, P. R. China
[2] Department of Mechanical Engineering, 2010 Black Engineering Building, Iowa State University, Ames, IA 50011, USA

An EMD model for nanocolloidal dispersions considering the interaction between atoms within solid particles is developed for viscosity calculation and studying the effect of the particle size and volume fraction. Strong oscillations are observed in the pressure tensor autocorrelation function. Elimination of this oscillation is achieved by adjusting the potential among atoms of nanoparticles to reduce the acoustic mismatch between particles and liquid. The shear viscosity of nanocolloidal dispersion is found strongly dependent on the particle size, which cannot be predicted by traditional effective medium theory. Through decomposing of the pressure tensor, the viscosity contribution from interactions between liquid–solid atoms and solid–solid atoms are believed to dominate the viscosity increase of colloidal systems. Our model reveals the shear viscosity increase mechanism at the molecular-level and predicts that the shear viscosity of simple colloidal dispersions reaches a plateau value when the particle size becomes large enough.

Keywords: Nanocolloid, Shear Viscosity, Molecular Dynamics, Stress Wave, Particle Size Effect.

1. INTRODUCTION

In recent years, attributed to the small size, large surface area, and significantly modified physical properties of nanoscale particles,[1–3] nanocolloidal dispersions have attracted considerable attention in applications related to cooling,[4] nanolubricant,[5] drug delivery and diagnosis.[6,7] In the aforementioned applications, the viscosity of nanocolloidal dispersions plays a critical role in the delivery system. For confined microfluids, the viscosity can differ remarkably from those of the corresponding bulk fluids.[8] Quite a lot of experimental work has been conducted to study the viscosity of nanocolloidal dispersions[9–13] and several expressions[11] have been proposed to express the effect of nanoparticle volume fraction on the viscosity of hard particle suspensions. However, various mechanisms of viscosity increase of nanocolloidal dispersions are proposed and the size effect of nanoparticle is not well revealed. The experimental work barely reveals the physics behind the viscosity increase of nanocolloidal dispersions. This is probably due to the extremely small size of particles and the difficulty in characterizing their dynamic rheological behavior. The interaction between particles and liquid significantly increases the difficulty in analytical/theoretical analysis of the viscosity of nanocolloidal dispersions. Moreover, when the particle moves in a complex structured environment such as blood, the situation becomes even more complicated.[14]

Motivated to study the physics underlying the shear viscosity of nanocolloidal dispersions, in this work a new EMD model considering the interaction among atoms of solid particles is developed and the viscosity contribution from particle size and volume fraction are investigated. Argon liquids consisting of nanoparticles of specially designed materials are studied. The stress wave scattering/reflection at the particle–liquid interface is found to give rise to the strong oscillation in the autocorrelation function of the pressure tensor. Elimination of this oscillation is achieved by reducing the acoustic mismatch between particles and liquid. Through decomposing the pressure tensor into potential and kinetic terms, the viscosity increase for nanocolloidal dispersions is investigated in detail.

Compared with experiments and theoretical analysis, molecular dynamics (MD) simulation provides a compelling way to evaluate/predict the macroscopic transport properties of fluids, like self diffusivity and shear viscosity. MD simulation directly tracks the movement of atoms and is able to provide unprecedented detail/information about the effect of particle size, volume fraction, particle shape, and agglomeration of particles on the viscosity of nanocolloidal dispersions. The interaction between particles and

*Authors to whom correspondence should be addressed.

liquid, including the information about the liquid layer adhering to particles as well as the effect of this layer on the viscosity, can also be revealed in great detail. There are two main categories of MD simulation for calculating shear viscosity: equilibrium MD (EMD) and nonequilibrium MD (NEMD). The NEMD techniques usually involve measuring the macroscopic steady-state response of a system to a perturbing field and relating the linear response to a transport coefficient (e.g., Sllod algorithm).[15, 16] McPhie et al.[17] used NEMD to study shear rate dependence of viscosity for solutions of model nanocolloidal particles. In their study, detailed information on changes in the viscosity of a nanocolloidal suspension was obtained as the hydrodynamic limit is approached. The zero shear rate viscosity was computed at different size ratios, mass ratios and volume concentrations and the results were compared with the theoretical relations based on the Einstein relation[18] $\eta = \eta_0(1+[\eta]\phi)$, where η and η_0 are the viscosity of colloidal dispersion and solvent, ϕ the volume fraction of solute and $[\eta]$ the intrinsic viscosity with the value of 2.5 for spherical particles. Recently a new method using momentum impulse relaxation was developed.[19] In this method, the shear viscosity is evaluated by fitting the decaying coarse-grain Gaussian velocity profile. One major drawback of NEMD is that the shear viscosity is wavelength or box-size dependent.[16] In our extensive attempt to use the momentum impulse relaxation method to calculate the shear viscosity of nanocolloidal dispersions, a very large system has to be used. This requires a very long computational time, especially for low viscosity systems whose velocity gradient decays very slowly.

EMD is a commonly used method by many researchers to study the self-diffusion coefficient and viscosity of nanocolloidal dispersions. The viscosity is determined from pressure tensor ($P_{\alpha\beta}$) fluctuations by using the Green-Kubo correlation.[20, 21] The advantage of EMD is its flexibility in the sense that a mixed system can be readily set up and more detail of transport coefficients or parameters, such as self-diffusion coefficient, shear viscosity or pressure tensor and stress wave propagation in the system can be studied. Nuevo et al.[22] used EMD to study the self-diffusion coefficient and shear viscosity of nanocolloidal dispersions. Their MD simulations were conducted at very high packing fractions (0.1–0.4). They used an empirical formula to interpret the concentration dependence of the viscosity. The results suggested that the volume fraction dependence of the Newtonian shear viscosity observed for macrocolloidal particle systems may extend largely unchanged down to simple liquid distance scales.[22] Bastea[23] used EMD to calculate the viscosity of a dilute colloidal suspension with colloidal particles roughly one order of magnitude larger than the suspending liquid molecules. The results showed the Einstein relation remained well applicable for predicting the shear viscosity when the mass of colloidal particles was much larger than that of the liquid molecules.

In the MD studies reviewed above, the researchers largely focused on the comparison between the simulated results and traditional hydrodynamic theory values. There are some basic differences between MD theory and hydrodynamic theory which make it difficult for conducting the comparison. Since the two theories are based on different assumptions and the studied objects are required to be ideal, either of them cannot predict the realistic colloidal system accurately. In MD simulation, the potential and motion of every molecule/atom are calculated accurately. The Einstein's equation is derived from hydrodynamic calculation in which rigid spheres, dilute suspension (no sphere–sphere interactions), no slip at the sphere-fluid interface, and no Brownian motion were assumed.[24] Although the Einstein's equation can be extended to higher volume fraction,[24] non-spherical particles,[25] and slip boundary condition,[26] it hardly deals with the strong Brownian motion of nanoparticles and the special interaction between solid particles and liquid molecules because of the large surface area of particles. McPhie et al.[17] tried to conduct MD simulations in the hydrodynamic limit and studied the agreement between the two theories. They suggested that due to the model interaction between solute and solvent particles in their MD system, the slip boundary condition was most appropriate. In order to accurately compare MD results with theoretical predictions under slip boundary condition, they used the concept of hydrodynamic volume fraction.

Although the comparisons are important and make a bridge between molecular level simulation and macroscopic theory, the details and physics underlying the viscosity increase of nanocolloidal dispersions are still not well explored, like the stress wave propagation and attenuation, as well as the stress wave scattering and diffraction at the particle–liquid interface. In EMD, the viscosity is determined from the autocorrelation function of pressure tensor by using the Green-Kubo correlation. The detail of pressure tensor and propagation of stress wave is important for understanding the viscosity of a mixture system. In the EMD simulations reviewed above, the Weeks-Chandler-Andersen (WCA) potential[17, 22, 23, 27] is commonly used between liquid atoms and solid particles, and no internal atom is configured in solid particles. One significant problem of this model is that no internal atomic/molecular interaction is considered within the colloid particles. This makes it difficult to explore stress tensor details, especially the stress wave propagation at the interface of solid–liquid and propagation within the particles. Using this EMD model, Nuevo et al.[22] found that the shear viscosity was subjected to great statistical uncertainty with increasing packing fraction and colloidal particle size. Quite often it was difficult to establish a plateau value in the integration of time correlation function and the value of the viscosity decreased with the increasing system size. In our EMD work on the viscosity of nanocolloidal dispersions, strong

oscillation in the autocorrelation function of the pressure tensor is observed while such phenomenon does not exist for pure fluids. The mechanisms of such oscillations need to be explored. Another problem of the WCA potential is that the interactions between the solvent and solute particles are purely repulsive and only slip boundary condition can be studied.

2. METHODOLOGIES OF SIMULATION

2.1. Basis About MD Simulation of Viscosity

The Lennard-Jones (LJ) potential (ϕ_{ij}) is applied in this work to describe the interatomic interactions for atoms inside solid particles, liquid atoms and the interaction between solid and liquid atoms. The interaction energy between atoms i and j, separated by a distance r_{ij}, is

$$\phi_{ij} = 4\varepsilon_m[(\sigma_m/r_{ij})^{12} - (\sigma_m/r_{ij})^6], \quad m = \mathrm{s, l, sl} \tag{1}$$

where ε and σ are the LJ well depth parameter and equilibrium separation parameter, respectively. The subscripts s and l denote solid and liquid atoms. For the liquid (solvent), the material takes argon. For the solid nanoparticle (spherical) material, it will use the LJ potential, but with varied atomic mass, well depth, and equilibrium separation (discussed later). The typical combining Berthelot geometric mean rule

$$\varepsilon_{\mathrm{sl}} = (\varepsilon_{\mathrm{s}} \cdot \varepsilon_{\mathrm{l}})^{1/2} \tag{2}$$

and Lorentz arithmetic mean combining rule

$$\sigma_{\mathrm{sl}} = (\sigma_{\mathrm{s}} + \sigma_{\mathrm{l}})/2 \tag{3}$$

are applied for the potential between solid and liquid atoms.[28] The cutoff distance for MD simulation takes 2.5 σ_{l} for liquid–liquid interaction, and 2.5 Max[σ_s, σ_{l}] for solid–solid and solid–liquid interactions. The half-step leap-frog scheme is used[21] in this work with a time step of 15 fs. Computation of the force between an atom and its neighbors is arranged by the cell structure and linked-list method.[21]

A MD program package developed by our group using FORTRAN is employed to conduct the simulation. For a dispersion system containing 27 nanoparticles with a diameter of 7 nm, a computational domain with a volume of 161,879 nm^3 and 3,526,656 atoms is needed if the volume fraction of particles is 3%. To reduce the computational time, parallel computation is employed through incorporating the programs with the message passing interface (MPI) program. As a result, the computational time for each step is about 5 second by using 4 CPUs, each of which has 4 cores. After initial configuration, the system is run for equilibrium calculation, after which the particle positions will change slightly due to Brownian motion.

In order to enhance the process of 'melting' for liquid argon at the initial stage of simulation, initially each argon atom is given a random Gaussian distribution velocity whose average is

$$\bar{v} = 2(k_{\mathrm{B}}T/m)^{1/2} \tag{4}$$

where T is the expected equilibrium temperature. In this work, we set the initial temperature as 143.4 K and the initial lattice constant a of crystalline argon at 0.5414 nm. After the argon melts, its density is 1.42 g $\cdot$ cm^{-3}.

The equilibrium simulation is performed for 7000 steps (~100 ps) to make the system reach the expected temperature. The velocity scaling is performed for the solid and liquid separately and simultaneously. After the equilibrium calculation, the pressure of the whole domain maintains at 1.5~1.6 $\times$ 10^8 Pa. Periodical boundary conditions are applied along the three directions of the computational domain.

In EMD, the viscosity of liquid (η) is determined by the Green-Kubo relation[20, 21]

$$\eta = V/(K_{\mathrm{B}}T)\int_0^\infty \langle P_{\alpha\beta}(0)P_{\alpha\beta}(t)\rangle dt \tag{5}$$

where V, K_{B} and T are volume, Boltzmann's constant and temperature, respectively. $P_{\alpha\beta}$ is an off-diagonal ($\alpha \neq \beta$) element of the pressure tensor given by

$$P_{\alpha\beta} = \left(\sum_{i=1}^{N} p_{i\alpha}p_{i\beta}/m_i + \sum_{i}^{N}\sum_{j>i}^{N} r_{ij\alpha}F_{ij\beta}\right)\Big/V \tag{6}$$

where N, p_i, r_{ij} and F_{ij} are the sum over all atoms, momentum vector for atom i, the vector connecting the centers of atoms i and j, and the force between them, respectively.

In order to achieve acceptable uncertainty, the EMD simulation for viscosity calculation needs to be performed for 150,000 steps (~2 ns) and the six pressure tensors P_{xx}, P_{yy}, P_{zz}, P_{xy}, P_{xz} and P_{yz} are calculated at each time step. In order to improve the statistical stability of the shear viscosity result from the Green-Kubo relation, all the six pressure tensors are used. Since the system is isotropic at equilibrium, we have[29]

$$P_{\alpha\beta} = P_{\beta\alpha} \tag{7}$$

Daivis et al.[30] have shown that the shear viscosity can then be calculated from the integral

$$\eta = V/(10K_{\mathrm{B}}T)\cdot\int_0^\infty \langle P^{os}(0)\colon P^{os}(t)\rangle dt \tag{8}$$

where P^{os} is the symmetrical traceless pressure tensor with components $P^{os}_{\alpha\beta}$ given by

$$P^{os}_{\alpha\beta} = (P_{\alpha\beta} + P_{\beta\alpha})/2 - \delta_{\alpha\beta}\left(\sum_{\gamma} P_{\gamma\gamma}/3\right) \tag{9}$$

RESEARCH ARTICLE

RESEARCH ARTICLE

2.2. Model Material Design to Eliminate Stress Wave Scattering at the Solid–Liquid Interface

Using the EMD model, Nuevo et al.[22] and our previous study both found strong oscillation in the pressure tensor autocorrelation function (PTACF). Figure 1 shows the oscillation of the PTACF of a nanocolloidal dispersion with 27 spherical nanoparticles. For this case, the diameter of particles is 7 nm and their volume fraction is 3%. This oscillation will introduce an obvious statistical error in viscosity calculation. It is well known that at the interface between dissimilar materials there will be an acoustic mismatch for sound wave propagation. The acoustic impedance mismatch of the two materials will introduce a weak transmission and strong reflection/scattering of stress wave at the interface as shown in Figure 2. The reflected or scattered stress wave from the interface will be reflected/scattered by other particle/liquid interfaces and forms oscillation in the liquid and solid. Model material of nanoparticles can be designed by changing the parameters of LJ potential to study the interaction between solid and liquid, effect of the particle density, as well as to eliminate the stress wave scattering at the solid–liquid interface. The design of new model material of nanoparticle will make the simulation more flexible to study the effect of intermolecular potential on viscosity without losing physical generality. The conclusion is generic and can be applied to a wide spectrum of materials.

The acoustic mismatch at the interface between dissimilar materials is determined by the acoustic impedance

$$Z = \rho \cdot c \tag{10}$$

where ρ and c are the mass density and speed of sound, respectively. For a stress wave/sound traveling to the interface between materials A and B, the transmission coefficient is

$$\alpha_{AB} = 4Z_A Z_B/(Z_A + Z_B)^2 \tag{11}$$

In order to make the acoustic impedance match, one way is to change the density of particles but not changing the sound speed inside. This can be realized by using different lattice constants for the solid material (a_s), but keeping the potential well depth and atomic mass constant. Such strategy is feasible based on the non-dimensional analysis. For a simple system governed by the LJ potential, the sound velocity is only a function of ε and m, and is proportional to $\sqrt{\varepsilon/m}$. It is clear that the sound will travel at the same speed in bulk solid materials of different lattice constants if the well depth parameter e and atomic mass m are kept constant. We have studied different systems of different lattice constants with the same ε and m. Indeed the sound wave is found constant regardless of the lattice constant.

In order to estimate to what extent the lattice constant should be adjusted, extensive additional NEMD simulations have been carried out to study the sound speed in bulk solid. Figures 3 and 4 show the stress wave propagation in solid and liquid material when a sudden force

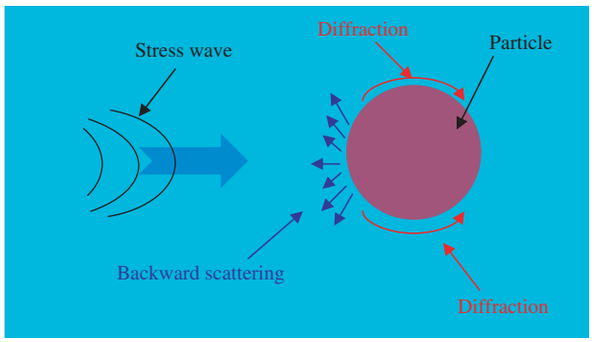

Fig. 2. Schematic of the stress wave propagation at the particle–liquid interface. The acoustic impedance mismatch will introduce strong scattering.

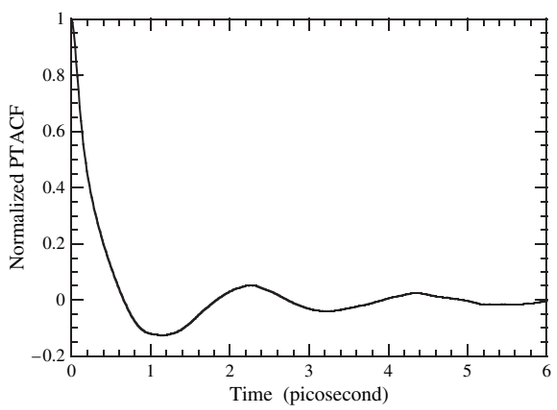

Fig. 1. Oscillation in PTACF for nanocolloidal dispersion with particles of 7 nm diameter and 3% volume fraction.

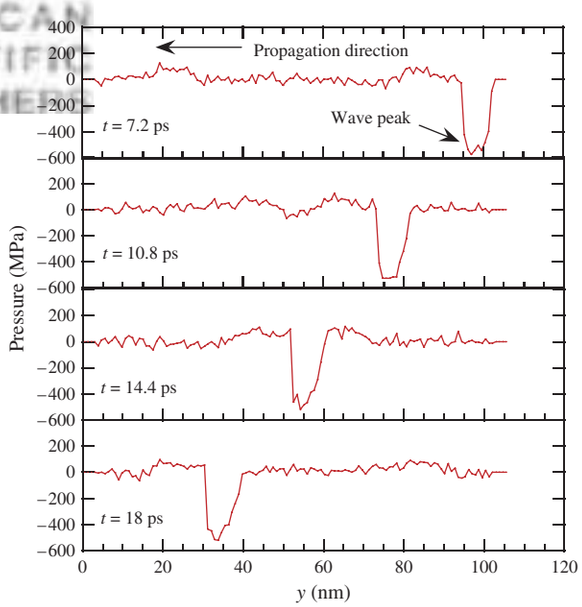

Fig. 3. The stress wave propagation in a solid material at 143.4 K. m_s/m_l takes 1 and the ε_s takes $16\varepsilon_l$.

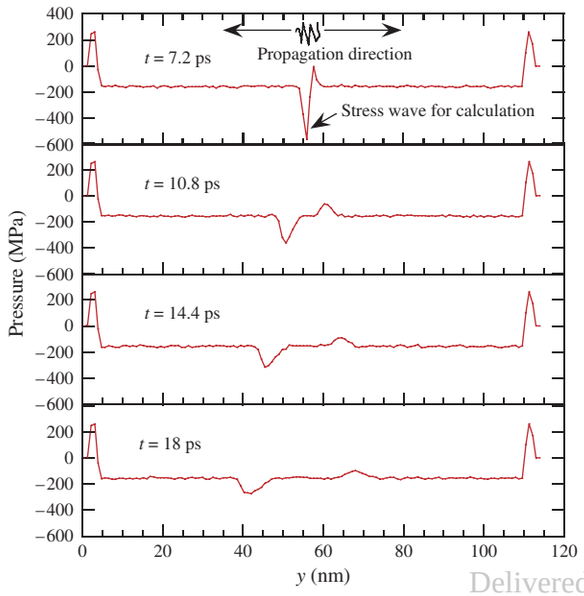

Fig. 4. The stress wave propagation in liquid argon at 143.4 K under pressure of $1.5\sim1.6\times10^8$ Pa.

applied at one end of the material in the [100] direction. The sound speed in bulk material can be calculated from the wave peak positions at different times. The simulations indicate that for the colloidal solid material at 143.4 K, the stress wave travels at a speed of 6280 $m\cdot s^{-1}$ in the [100] direction when m_s/m_l takes 1 and the ε_s takes $16\varepsilon_l$. For liquid argon at 143.4 K under pressure of $1.5\sim1.6\times10^8$ Pa, the stress wave travels at a speed of 1190 $m\cdot s^{-1}$. In order to make the acoustic impedance of the two materials the same, the colloidal particle needs to have a smaller density, corresponding to a lattice constant of $1.7a_{Ar}$. Figure 5 shows the effect of lattice constant on the oscillation of PTACF. The volume fraction of colloidal

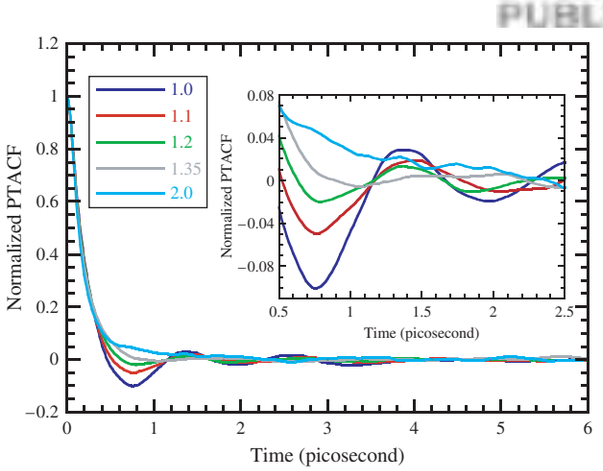

Fig. 5. The PTACF of nanocolloidal dispersions with different lattice constants for colloidal particles. The numbers shown in the figure is a_s/a_{Ar}. The volume fraction of colloidal particles is 3%, m_s/m_l takes 1, the particle radius is 2 nm, and ε_s takes $16\varepsilon_l$ for all the cases.

particles is 3%, m_s/m_l takes 1, the particle radius is 2 nm, and ε_s takes $16\varepsilon_l$ for all the cases. In order to keep the system stable, the equilibrium separation (σ_s) and the lattice constant of the model solid material are extended with the same coefficient. From Figure 5 it is observed as the lattice constant of the solid particle is larger (less dense for the particle), the negative peak of PTACF curves decays very quickly with the decreasing density. When a_s/a_{Ar} is 1.35, the PTACF curve is already quite smooth without visible oscillation, meaning the reflection/scattering of the stress wave at the solid–liquid interface is substantially weak. This strategy of suppressing the stress wave scattering at the solid–liquid interface and eliminating the oscillation in the PTACF by adjusting the lattice constant of solid material will be implemented in our viscosity studies. It is worth noting that the acoustic impedance adjustment is realistic. Although by now, we cannot change the lattice constant of a crystal material, the acoustic impedance can be adjusted by other experimental methods, like gradient coating on the nanoparticle.

2.3. Contributions to Viscosity Increase of Nanocolloids from Different Mechanisms

In hydrodynamic theories, the viscosity increase of colloids is contributed from volume fraction and shape of solute particles. For an EMD system, one has the following form in Eq. (12) which shows two terms, the kinetic (K) and the potential (P) that constitute the pressure tensor:

$$P_{\alpha\beta}=\left(\sum_{i=1}^{N}\underbrace{p_{i\alpha}p_{i\beta}/m_i}_{K}+\sum_{i}^{N}\sum_{j>i}^{N}\underbrace{r_{ij\alpha}F_{ij\beta}}_{P}\right)\Big/V \qquad (12)$$

Consequently, the viscosity can be expressed as a sum of two terms which can be conveniently grouped together into self correlations, KK, PP and two cross correlations KP, PK. For convenient decomposition and comparison, only pressure tensor in the $x-y$ plane is analyzed, and Eqs. (5) and (6) are employed in the following results and discussions. Figure 6 illustrates the normalized press tensor autocorrelation function (PTACF) for shear viscosity of pure Ar liquid at 143.4 K and contributions from KK, PP and cross terms. Figure 7 shows the time of integrals of the shear viscosity for pure Ar liquid and contributions from partial terms. The plateau in the running integral of viscosity signifies that the corresponding PTACF has decayed to zero and is fluctuating along the horizontal time axis. Longer correlation times will have larger statistical uncertainty because less data are available for its calculation. As shown in Figure 6, the PTACF reaches zero at about 1.1 ps, so we can determine the shear viscosity and contributions from different terms using the values of their running integrals at this time. It is clear that the kinetic–kinetic (KK) and kinetic–potential (KP) functions contribute only in the order of a few percentage (about 7%) to the total viscosity,

RESEARCH ARTICLE

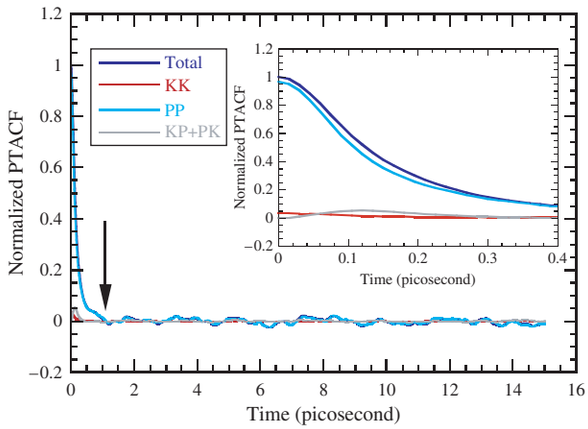

Fig. 6. The PTACF for pure Ar liquid (143.4 K and $1.5\sim1.6\times10^8$ Pa) and contributions from KK, PP and cross terms, which shows that the PTACF decays to zero at about 1.1 ps (marked by the arrow). The inset is an enlarged view between 0 ps and 0.4 ps.

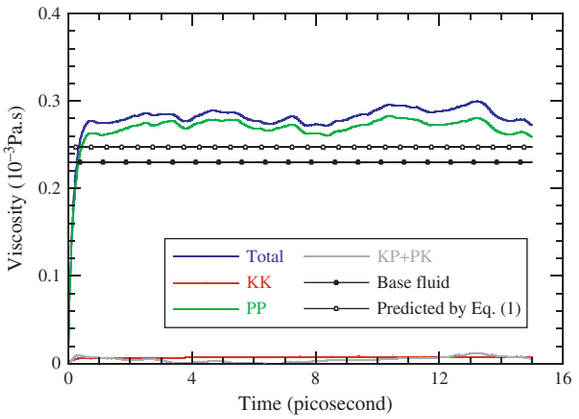

Fig. 8. The viscosity of nanocolloidal dispersion (4 nm diameter, 3 vol.%) and contributions from KK, PP and cross items. The solid line is the viscosity value of base fluid (Ar, 143.4 K) and the dashed line is the predicted value using the Einstein relation for colloidal dispersion.

while the potential–potential (PP) term dominantly contributes to the total PTACF (about 93%). Figure 8 shows the running integrals of the shear viscosity for one kind of nanocolloidal dispersion and the contributions from partial terms. The volume fraction of colloidal particles is 3%, m_s/m_l takes 1, the particle diameter is 4 nm, ε_s takes $16\varepsilon_l$, and the lattice constant is extended to 1.35 α_{Ar}. The viscosity can be determined at 0.75 ps. The viscosity of colloidal dispersion also has a dominant contribution of about 93% from PP. The KK and cross terms account for the remaining 7%.

In Figure 8, the viscosity increase of colloidal dispersion relative to the base fluid (Ar, 143.4 K, $\eta = 0.23\times10^{-3}$ Pa·s) has a dominant contribution from PP. Meanwhile, the total viscosity increase is significantly higher than the prediction of the Einstein relation with $[\eta]$ being 2.5 for spherical particles. For a colloidal system, the potential term from the pressure tensor can be further decomposed into three terms: the potential between liquid–liquid atoms (P_{ll}), the potential between solid–solid atoms (P_{ss}) and the potential between liquid–solid atoms (P_{ls})

$$\sum_i^N\sum_{j>i}^N \underbrace{r_{ij\alpha}F_{ij\beta}}_{P} = \sum_i^{N_l}\sum_{j>i}^{N_l} \underbrace{r_{ij\alpha}F_{ij\beta}}_{P_{ll}} + \sum_i^{N_s}\sum_{j>i}^{N_s} \underbrace{r_{ij\alpha}F_{ij\beta}}_{P_{ss}} + \sum_i^{N_l}\sum_{j}^{N_s} \underbrace{r_{ij\alpha}F_{ij\beta}}_{P_{ls}} \quad (13)$$

where N_l and N_s are the sum over all liquid atoms and all solid atoms, respectively. Consequently, the contribution from PP can be expressed as a sum of three terms which can be grouped together into self correlations PP_{ll}, PP_{ss}, PP_{ls} and six cross correlations PP_{l-s}, PP_{l-ls}, PP_{s-ls}, PP_{s-l}, PP_{ls-l}, PP_{ls-s}. The decomposing results of PP from Figure 8 are shown in Figure 9. The viscosity value contributed by

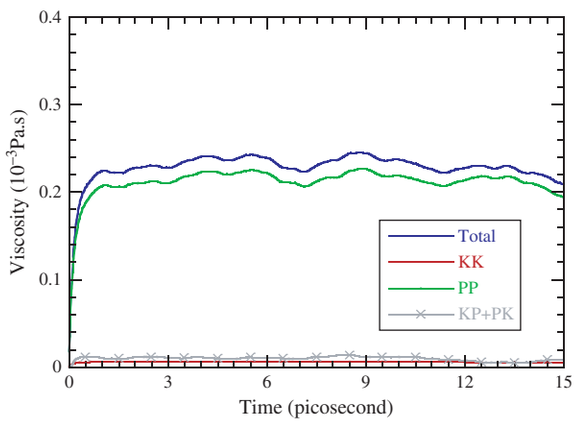

Fig. 7. The viscosity of pure Ar liquid (143.4 K and $1.5\sim1.6\times10^8$ Pa) and contributions from KK, PP and cross terms.

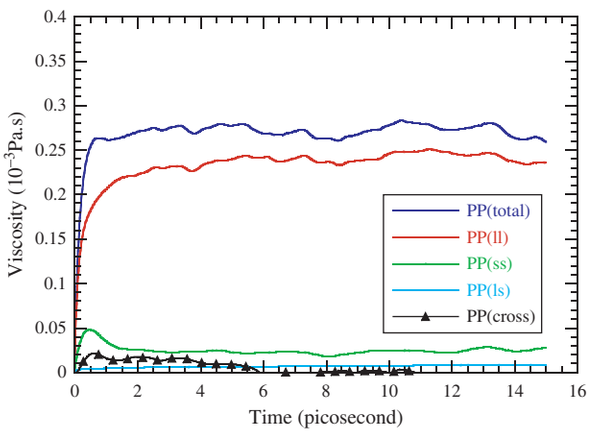

Fig. 9. The viscosity contributions from potential of nanocolloidal dispersion (4 nm diameter, 3 vol.%). The PP cross term includes all the contribution from PP_{l-s}, PP_{l-ls}, PP_{s-ls}, PP_{s-l}, PP_{ls-l}, PP_{ls-s}.

RESEARCH ARTICLE

interaction between liquid atoms (PP_{ll}) has a reasonable level close to that of pure Ar liquid. The primary viscosity increase comes from the sum of PP_{ss}, PP_{ls} and cross terms. The dominant contribution will be studied through more detailed decomposing of potential terms in Section 3. Since the interaction between liquid and solid atoms (PP_{ls}) and interaction between solid atoms (PP_{ss}) are two important components, the particle size and volume fraction will be varied to study their contributions to viscosity increase.

3. RESULTS AND DISCUSSION

In this work, the simulation box consists of two sub-domains. One sub-domain is the solid particles which are dispersed in a box. The spherical nanoscale solid particles are dispersed uniformly and the distance between particles is set the same initially. Figure 10 shows the configuration of dispersed nanoparticles at the beginning of simulation. m_s/m_l takes 1, ε_s takes $16\varepsilon_l$ and the lattice constant of solid particle is extended to 1.35 α_{Ar} for all the cases.

3.1. Effect of Particle Size on Viscosity

Figure 11 shows the particle size effect on viscosity of nanocolloidal dispersions. The volume fraction of solid particles is all kept at 3%. The viscosity values calculated by MD and Einstein models are listed in Table I. Except that the MD value at 4 nm is smaller than that at 3 nm (probably due to statistical fluctuation), the trend of viscosity increase with the increasing particle size is clear. Table I also shows that the viscosity at 2 nm is already higher than the Einstein value and the Einstein relation cannot predict the size effect.

As discussed in part C of Section 2, the viscosity increase of nanocolloidal dispersions primarily comes from the increase in the PP correlation. For colloid systems, the interactions between atoms can be strongly affected by the large surface area of nanoscale solid particles. At the same volume fraction, for smaller particles, the number of interacting pairs of liquid–solid atoms will increase and the number of interacting pairs of solid–solid atoms will decrease, which can further change the viscosity contributions from PP_{ls} and PP_{ss}. Figure 11 plots the decomposing results of PP at different particle sizes and the viscosity increase with respect to the Einstein relation. The PP_{ss} increases with the increasing particle size. In contrast, the PP_{ll} maintains at the level of pure base fluid and the PP_{ls} and cross components are very small for all particle sizes. One important feature of the decomposing results is that the curve of PP_{ss} nearly overlaps with that of the viscosity increase with respect to the Einstein prediction, which explains the anomalous viscosity increase with increasing particle size is probably due to the potential interaction between solid atoms. Another interesting phenomenon is that there is a slight decrease of PP_{ls} with increasing particle size, which could be due to the decreasing specific surface area of particles. In order to further study the mechanism of the anomalous viscosity change, especially the contributions from interactions between different kinds of atoms, the effect of volume fraction on viscosity is studied. Figure 11 indicates that with the decrease of particle size, the viscosity of the nanocolloidal dispersion is decreasing. This is physically reasonable. One extreme situation will be that when the particle only consists of a single atom, it will be more like a mixture of two

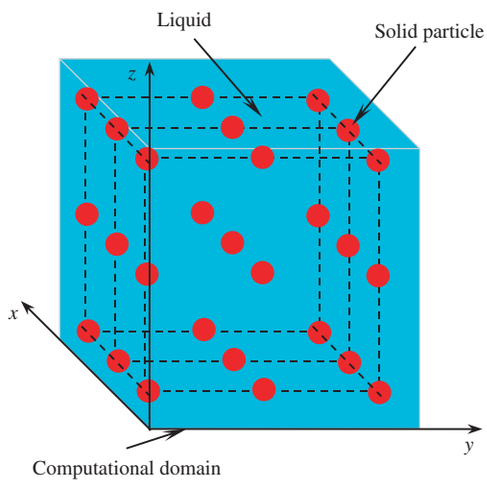

Fig. 10. Schematic of the computational domain and initial particle configuration.

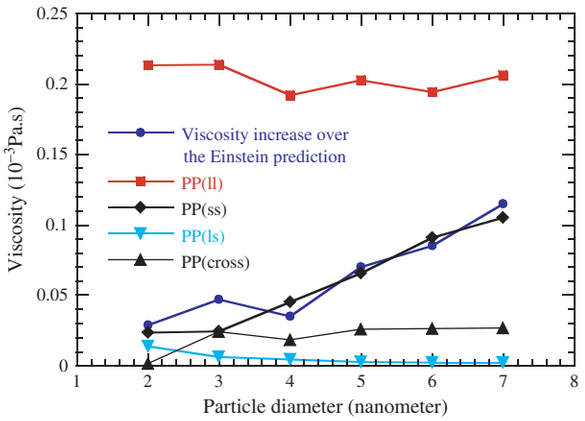

Fig. 11. The decomposing result of PP at different particle diameters (3% volume fraction).

Table I. Shear viscosity values at different particle size (3 vol.%).

Particle size (diameter)	2 nm	3 nm	4 nm	5 nm	6 nm	7 nm
Shear viscosity, MD model (10^{-3} Pa·s)	0.277	0.295	0.283	0.318	0.333	0.363
Shear viscosity, Einstein model (10^{-3} Pa·s)	0.248	0.248	0.248	0.248	0.248	0.248

RESEARCH ARTICLE

different liquids, and the viscosity increase will be very much limited.

3.2. Effect of Volume Fraction on Viscosity

Table II shows the viscosity of nanocolloidal dispersions at different volume fractions. The diameters of solid particles in different cases are all kept 4 nm. The viscosity is determined at the time when PTACF reaches zero. The shear viscosity calculated by our MD model increases obviously with the increasing volume fraction, except the case at 1% volume fraction due to statistical uncertainty. The viscosity has a dominant contribution of more than 93% from PP. The viscosity value by the Einstein relation is also listed in Table II, which is significantly lower than the corresponding MD result. Meanwhile, the average nearest distance between particle surfaces is calculated and listed in Table II. The distance decreases quickly with the increasing particle volume fraction. When the volume fraction is larger than 5%, the nearest distance between particle surfaces is already smaller than the particle diameter. Considering the distance is still larger than the cutoff distance ($r_{cut} = 2.5\sigma$), there would be no direct molecular interaction between particles.

Figure 12 shows the decomposing results of PP at different volume fractions. The PP_{ll} still maintains at the level of pure base fluid for different volume fractions. The PP_{ss} increases quickly with the increasing volume fraction, and for volume fraction more than 9%, the contribution from PP_{ss} is even comparable to or larger than that from PP_{ll}. The increase of PP_{ss} can be simply explained as this: with volume fraction increasing, more particles are contained in the system and more solid atoms which can interact with each other are contained in the system. Different from Figure 11, there is an obvious increase for viscosity contribution from cross components with increasing volume fraction. This is related with the strong volume fraction effect of potential between solid atoms through Eq. (13). Another feature different from Figure 11 is that the interaction between liquid and solid atoms increases slightly with increasing volume fraction, which should be due to the increasing total surface area of particles. This explains the increase of PP_{ls} with the volume fraction as shown in Figure 12. The most interesting phenomenon is that the curve of PP_{ss} also nearly overlaps with that of the unexpected viscosity increase, as shown in Figure 12. This again confirms that the anomalous viscosity increase with increasing volume fraction should be due to the interactions between solid atoms.

Table II. Shear viscosity values at different volume fractions (4 nm diameter).

Volume fraction of particles	0.5%	1%	3%	5%	7%	9%
Shear viscosity, MD model (10^{-3} Pa·s)	0.252	0.251	0.283	0.347	0.367	0.456
Shear viscosity, Einstein model (10^{-3} Pa·s)	0.233	0.236	0.247	0.259	0.270	0.282
Viscosity contributed by PP (10^{-3} Pa·s)	0.237	0.232	0.263	0.328	0.350	0.438
Average distance between particle surfaces (nm)	14.9	11.0	6.4	4.7	3.8	3.2

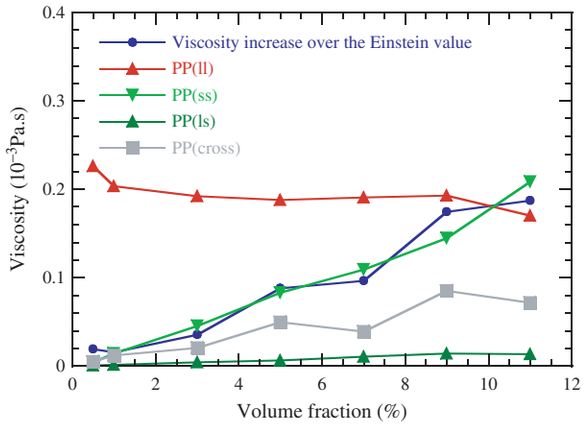

Fig. 12. The decomposing result of PP at different particle volume fractions (4 nm diameter).

3.3. Mechanism of Viscosity Increase

The anomalous viscosity increase for nanocolloidal dispersions in comparison with the Einstein value shown in the above MD simulation results is rarely studied in the past. In the EMD simulation, the viscosity of nanocolloidal dispersion contributed by the potential term can be expressed as:

$$\eta(P) = \eta(P_{ll}) + \eta(P_{ls}) + [\eta(P_{ss}) + \eta(\text{cross})] \qquad (14)$$

In comparison with the Einstein equation, the viscosity contribution $[\eta(P_{ss}) + \eta(\text{cross})]$ by interactions between solid atoms and the cross components are not considered by the Einstein theory. Viscosity is a transport property which reflects the capability of the system for transferring momentum. In statistical mechanical theory of transport, the stress tensor is contributed by the intermolecular force, and the interactions between species should be considered in the viscosity calculation. Another difference between our EMD results and the Einstein theory is that the viscosity is not only affected by the volume fraction of solute, but also affected by the particle size. The special characters of nanoparticles, like the finite size and large fraction of surface atoms are expected to play important roles in the mechanism of viscosity increase.

In the above simulation results, $\eta(P_{ss})$ dominates the anomalous viscosity increase. From Eqs. (5) and (6) we know that besides the surroundings, there are two factors which can affect the viscosity contribution from PP_{ss}: parameters of LJ potential and number of interaction atomic pairs per volume (NAPPV, $\tilde{n}$) for solid atoms. The

potential parameters of nanoparticles are all kept the same for our viscosity calculation reported above. Owing to the finite size and large volume fraction of surface atoms in nanoparticles, the number of interacting atom pairs per particle volume can be expressed as a ratio of the number of interaction pairs over the particle volume. The atomic pair distribution function analysis can be applied to determine $\tilde{n}$. The pair distribution function is usually employed to study the structure of material by calculating the probability of occurrence of an atom at a distance r from another one. The number of pair atoms in a shell of thickness dr at distance r from another one are obtained as $g(r)dr$, where $g(r)$ is the radial distribution function and can be expressed below for nanoparticles:[31]

$$g(r,D)=\pi r^2\rho_0'[2(r/D)^3-6(r/D)+4] \quad (r\le D) \quad (15)$$

where ρ' is the atomic number density of the nanoparticle. Since only atoms which have distance within the cutoff distance (r_{cut}) are considered in the potential calculation, the total number of interacting atom pairs in a nanoparticle is the integral result of $g(r, D)$ with r varies from 0 to r_{cut}:

$$N(D)=(N_0/2)\int_0^{r_{cut}} R(r,D)dr \quad (16)$$

where N_0 is the total atomic number in the nanoparticle, and $\tilde{n}=N(D)/\text{Volume}(D)$. Combining Eqs. (15) and (16), we have

$$\tilde{n}=\pi(\rho_0')^2[r_{cut}^6/6D^3-3r_{cut}^4/4D+2r_{cut}^3/3] \quad (17)$$

It is clear $\tilde{n}$ will increase with increasing diameter and reach a plateau value when the diameter is large enough. The normalized results of $\tilde{n}$ from MD model and Eq. (17) are shown in Figure 13, and the size effect is very obvious. There is a little difference between the two models because the radial distribution function is a continuous function in numerical calculation and discrete in MD simulation. This makes the interacting atomic pair number in MD a little smaller than that of numerical calculation. But

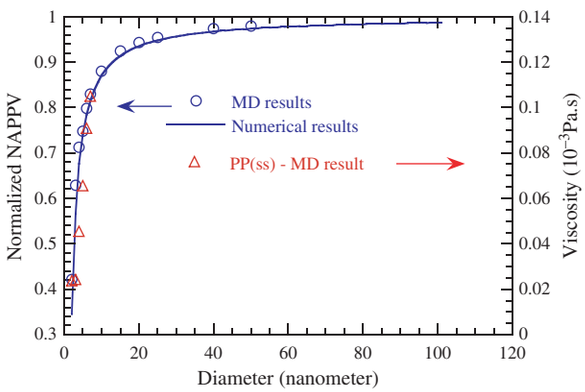

Fig. 13. The normalized NAPPV and its relation with viscosity increase contributed from interaction between solid atoms.

the NAPPV results after normalization agrees well with each other. In order to show the idea of NAPPV effect on viscosity increase, the viscosity contribution from PP_{ss} is also shown in Figure 13. It is evident that the PP_{ss} follows the same trend as the NAPPV. It can be concluded that, at nanoscales (less than 20 nm), the anomalous viscosity increase from PP_{ss} is mainly due to the increasing number of interacting atom pairs per particle volume. Although the MD calculation can hardly process such a huge domain, we can still project that the viscosity contribution from PP_{ss} will reach a plateau value (about 0.135×10^{-3} Pa·s) when the particle diameter is larger than 100 nm.

Besides PP_{ss}, other components also will be affected by the NAPPV. The PP_{ls} is strongly related to the interaction between liquid atoms and solid atoms. The NAPPV of liquid–solid will decrease with the increasing particle size because of the decreasing volume fraction of surface atoms. The slight decrease of viscosity contributed from PP_{ls} in Figure 11 confirms this projection. In traditional effective medium theory, the viscosity increase from volume fraction of solid particles is related to the interaction between liquid and solid, which can be regarded as the contribution from PP_{ls}. MD simulations using modified WCA potential[17, 22, 23] all obtained results that the effective medium theories remain well applicable for predicting the shear viscosity under hydrodynamic conditions. Since in those models no internal atomic/molecular interaction is considered within the colloid particles, the viscosity contributed from PP_{ls} is believed to dominate the viscosity increase and be consistent with the Einstein relation for dilute dispersion. In our MD model, not only the PP_{ls} is related with the volume fraction, the viscosity contribution from PP_{ss} increases linearly with increasing volume fraction because of the increasing NAPPV (solid–solid). This can be seen in Figure 12, and the viscosity contribution from PP_{ll} will decrease with increasing volume fraction of colloid particles.

Figure 13 reveals that the number of interacting atom pairs per volume, which will be affected by volume fraction and size of particles, is believed to be the mechanism of viscosity increase. There is a characteristic size at which the NAPPV will reach a plateau value. For nanoscale particles whose diameter is smaller than the characteristic size, the viscosity contribution from interaction between solid atoms will be strongly affected by the particle size. Although extensive experimental results about nanocolloidal viscosity have been published[9, 11] and no obvious size effect is revealed,[32] the agglomerations of nanoparticles in the dispersion can hardly be avoided and the interactions between molecules/atoms will be affected a lot by the structure of particle clusters, like the size, shape and compactness. Our model also predicts that when the particle size approaches microscale or macroscale, the viscosity increase will only be affected by the volume fraction of particles, which is consistent with the traditional effective medium theory.

In this paper, the objective of lattice constant adjustment for solid particles is to make the acoustic impedance match at the solid–liquid interface, thereby eliminating the stress wave oscillation. The lattice constant adjustment means adjustment of lattice structure, and possibly it will influence the viscosity of the entire system. One extreme situation will be that with a certain weak potential, the particles become so 'soft' that they cannot keep a stable shape in the solution. The solution will be more like a liquid–liquid mixture, and will have different viscosity compared to that with hard particles. In this paper, the potential between solid atoms is set and not changed with particle size or volume fraction. The studied nanoparticles have the same lattice constant ($1.35\alpha_{Ar}$), the observed general trend about the size effect on viscosity will not be influenced by the lattice constant adjustment.

4. CONCLUSION

In summary, EMD simulations were conducted to explore the mechanism of viscosity increase for nanocolloidal dispersions. An EMD model with considering the interaction between atoms within solid particles was developed and the particle size and volume fraction effect on viscosity increase was investigated. The stress wave scattering/reflection at the particle–liquid interface was found to give rise to the strong oscillation in the PTACF. Elimination of this oscillation was achieved by adjusting the potential among atoms within nanoparticles to reduce the acoustic mismatch between particles and liquid. The EMD calculation results showed that the shear viscosity of nanocolloidal dispersions was strongly dependent on the particle size, which cannot be predicted by the traditional effective medium theory. Through decomposing of the pressure tensor, the potential interaction between solid atoms was found to dominate the anomalous viscosity increase. The atomic pair distribution function was employed to study the particle size effect on the interaction between atoms. The number of interacting atom pairs per volume was believed to be the mechanism of viscosity increase. When the particle size is smaller than a characteristic size, the viscosity will be affected by particle size obviously and when the particle size approaches microscale or macroscale, no size effect will be observed.

Acknowledgments: Partial support from the start-up fund of Iowa State University is gratefully acknowledged. The authors especially appreciate the strong support from the National Natural Science Foundation of China (50676082), China Postdoctoral Science Foundation (20080441248) and Research Foundation of Science and Technology Department of Zhejiang Province, China (2009C21023).

References and Notes

1. J. Rupp and R. Birringer, *Phys. Rev. B* 36, 7888 **(1987)**.
2. H. Gleiter, *Prog. Mater. Sci.* 33, 223 **(1989)**.
3. H. Zhang and J. F. Banfield, *J. Mater. Chem.* 8, 2073 **(1998)**.
4. J. A. Eastman, S. U. S. Choi, S. Li, W. Yu, and L. J. Thompson, *Appl. Phys. Lett.* 78, 718 **(2001)**.
5. F. D. S. Marquis and L. P. F. Chibante, *JOM* 57, 32 **(2005)**.
6. S. Jin and K. Ye, *Biotechnol. Prog.* 23, 32 **(2007)**.
7. A. Komoto and S. Maenosono, *J. Chem. Phys.* 125, 114705 **(2006)**.
8. J. Zhang, B. D. Todd, and K. P. Travis, *J. Chem. Phys.* 121, 10778 **(2004)**.
9. J. Yamanaka, N. Ise, H. Miyoshi, and T. Yamaguchi, *Phys. Rev. E* 51, 1276 **(1995)**.
10. X. Wang, X. Xu, and S. U. S. Choi, *J. Thermophys. Heat Trans.* 13, 474 **(1999)**.
11. F. J. Rubio-Hernandez, M. F. Ayucar-Rubio, J. F. Velazquez-Navarro, and F. J. Galindo-Rosales, *J. Colloid Interface Sci.* 298, 967 **(2006)**.
12. N. Putra, W. Roetzel, and S. K. Das, *Heat Mass Trans.* 39, 775 **(2003)**.
13. B. C. Pak and Y. I. Cho, *Exp. Heat Trans.* 11, 151 **(1998)**.
14. M. Kim, D. Kim, S. Lee, M. S. Amin, I. Park, C. Kim, and M. Zahn, *IEEE Transactions on Magnetics* 42, 979 **(2006)**.
15. D. J. Evans and G. P. Morris, Statistical Mechanics of Nonequilibrium Liquids, Academic, London **(1990)**.
16. B. Hess, *J. Chem. Phys.* 116, 209 **(2002)**.
17. M. G. McPhie, P. J. Daivis, and I. K. Snook, *Phys. Rev. B* 74, 031201 **(2006)**.
18. A. Einstein, *Ann. Phys.* 34, 591 **(1911)**.
19. G. Arya, E. J. Maginn, and H.-C. Chang, *J. Chem. Phys.* 113, 2079 **(2000)**.
20. R. Zwanzig and R. D. Mountain, *J. Chem. Phys.* 43, 4464 **(1965)**.
21. M. P. Allen and D. J. Tildesley, Computer Simulations of Liquids, Clarendon, Oxford **(1987)**.
22. M. J. Nuevo, J. J. Morales, and D. M. Heyes, *Phys. Rev. E* 58, 5845 **(1998)**.
23. S. Bastea, *Phys. Rev. B* 75, 031201 **(2007)**.
24. C. Hsueh and P. F. Becher, *J. Am. Ceram. Soc.* 88, 1046 **(2005)**.
25. Y. Sun, X. Li, N. Duzgunesv, Y. Takaoka, S. Ohi, and S. Hirota, *Biophys. J.* 85, 1223 **(2003)**.
26. E. Wajnryb and J. S. Dahler, *Physica A* 253, 77 **(1998)**.
27. J. R. Schmidt and J. L. Skinner, *J. Chem. Phys.* 119, 8062 **(2003)**.
28. R. L. Scott and D. V. Fenby, *Annu. Rev. Phys. Chem.* 20, 111 **(1969)**.
29. L. I. Kioupis and E. J. Maginn, *Chem. Eng. J.* 74, 129 **(1999)**.
30. P. J. Daivis and D. J. Evans, *J. Chem. Phys.* 100, 541 **(1994)**.
31. K. Kodama, S. Iikubo, T. Taguchi, and S. Shamoto, *Acta Cryst. A* 62, 444 **(2006)**.
32. R. Prasher, D. Song, J. Wang, and P. Phelan. *Appl. Phys. Lett.* 89, 133108 **(2006)**.

Received: 16 November 2009. Accepted: 4 June 2010.